A VSS Speed Controller With Model Reference Response for Induction Motor Drive

Chang-Ming Liaw, *Member, IEEE,* Yeong-May Lin, and Kuei-Hsiang Chao

***Abstract*—This paper is mainly concerned with the development of a variable-structure system (VSS) controller with model reference speed response for an induction motor drive. An indirect-field-oriented (IFO) induction motor drive is first implemented, and its dynamic model at a nominal operating condition is estimated from measured data. Then, a two-degrees-of-freedom linear model-following controller (2DOFLMFC) is designed to meet the prescribed tracking and load regulation speed responses at the nominal case. As the variations of system parameters and operating condition occur, the prescribed control specifications may not be satisfied further. To improve this, a VSS controller is developed to generate a compensation control signal to reduce the control performance degradation. The proposed VSS controller is easy to implement, since only the output variable is sensed. The existence condition of sliding-mode control is derived, and the chattering suppression during the static period is also considered. Good model-following tracking and load regulation speed responses are obtained by the designed VSS controller. Effectiveness of the proposed controller and the performance of the resulting drive system are confirmed by some simulation and measured results.**

***Index Terms*—Chattering suppression, induction motor, model reference control, speed control, variable-structure system.**

I. Introduction

IT IS KNOWN that indirect-field-oriented (IFO) control has made the induction motor possess torque-generating capability like a dc motor, and it has been successfully employed in many industry applications. However, its decoupling characteristic is highly sensitive to the rotor parameters [1]. If the rotor parameters set in the field-orientation scheme cannot be tuned according to their actual values, the torque-generating characteristics will become sluggish and oscillatory. Although many control strategies have been proposed [2], [3] to make the tuning of the field-orientation mechanism for obtaining better decoupling characteristics, the success in ideal decoupling is still limited. It follows that the development of sophisticated control techniques to improve the control performance of the detuned IFO induction motor drive is very important.

A high-performance speed motor drive should possess good command tracking and load regulation dynamic responses, and these responses should be insensitive to the operating condition and the parameter variations. The proportional (P), proportional plus integral (PI), IP, proportional plus integral plus derivative (PID), I-PD, and PI-D conventional controllers are very easy to design and implement, but can obtain only the compromised tracking and regulation responses owing to their one-degree-of-freedom (1DOF) structure. A 2DOF controller and its systematic design procedure developed in [4] has been successfully incorporated the quantitative tracking and regulation control specifications into the design of controller. Based on this type of 2DOF controller, some modified controllers were proposed [5], [6] to let the motor drive preserve the prescribed drive specifications as the system parameters and operation conditions are changed. In addition to these, many other advanced control techniques have also been developed in the past years for the speed control of induction motor drives, see for example, the optimal control in [7], adaptive control in [1], [8], robust control in [9], variable-structure system (VSS) control in [10] and [11], and intelligent control in [5], [6], and [12].

It is known that the VSS control is one of the most effective methods to reduce the performance degradation due to large system parameter changes and disturbances. Generally speaking, the VSS controller has some limitations: 1) all system states should be accessible; 2) like the fuzzy logic controller [13], it possesses the inherent chattering problem; this high-frequency switching phenomenon will result in large control energy dissipation and large noise and, moreover, it may also excite the unmodeled dynamics causing stability problems; and 3) the tracking and regulation responses are rather difficult to be quantitatively achieved simultaneously; the chattering occurs mainly due to the switching with infinite speed can not be fulfilled. Much research [11], [14], [15] has been focused on eliminating or reducing the chattering effects. These can be roughly classified into two types. In the first type, the sign function used in the control law is replaced with some kinds of continuous functions [11], [14]. As to the second type, the chattering is reduced through tuning the parameters of the control law [15]. Recently, intelligent control has been widely applied to many control applications. A combination of fuzzy control and sliding-mode control, called fuzzy sliding-mode control [13], is a simple and effective approach. It can satisfy both the requirements of robustness and chattering reduction. In addition, some variable-structure model reference adaptive controllers (VS-MRAC) have also been proposed [16], [17]. They are simple to implement since only the input and output measurements are needed.

In this paper, a VSS controller is developed for the speed control of an IFO induction motor drive. First, a 2DOF model-fol-

Manuscript received March 29, 1999; revised June 1, 2001. Abstract published on the Internet October 24, 2001. This work was supported by the National Science Council, Taiwan, R.O.C., under Grant NSC-85-2213-E-007-038.

C.-M. Liaw is with the Department of Electrical Engineering, National Tsing Hua University, Hsinchu 300, Taiwan, R.O.C. (e-mail: cmliaw@ee.nthu.edu.tw).

Y.-M. Lin is with the R&D Department, AMBIT Microsystems Corporation, Hsinchu 300, Taiwan, R.O.C.

K.-H. Chao is with the Department of Electrical Engineering, National Chin Yi Institute of Technology, Taichung 411, Taiwan, R.O.C.

Publisher Item Identifier S 0278-0046(01)10286-8.

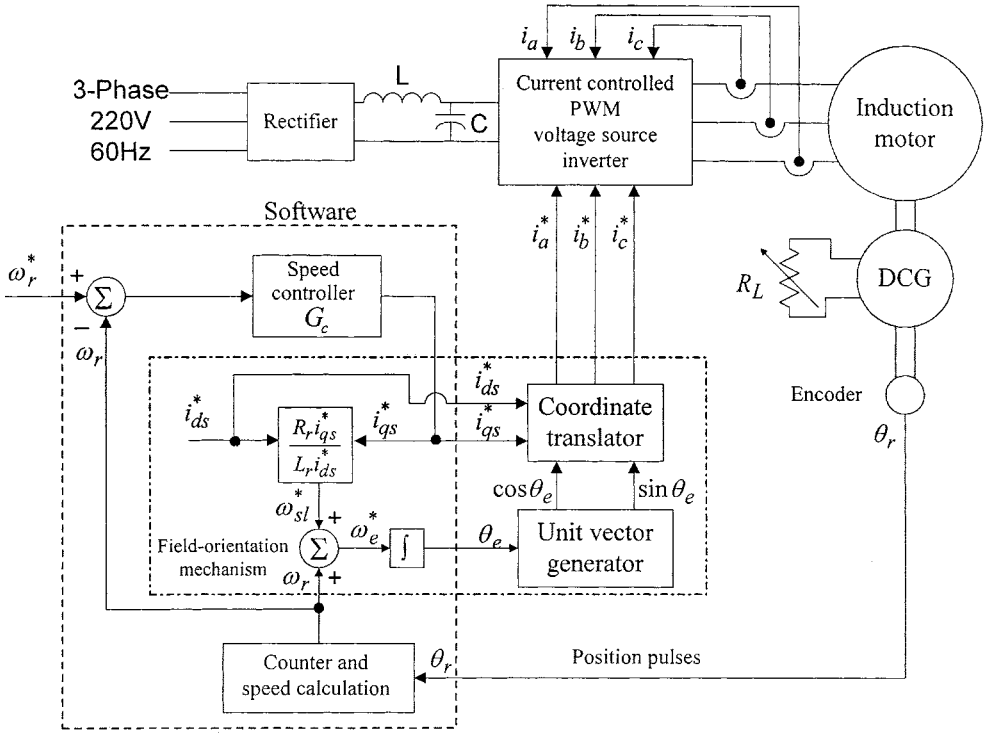

(a)

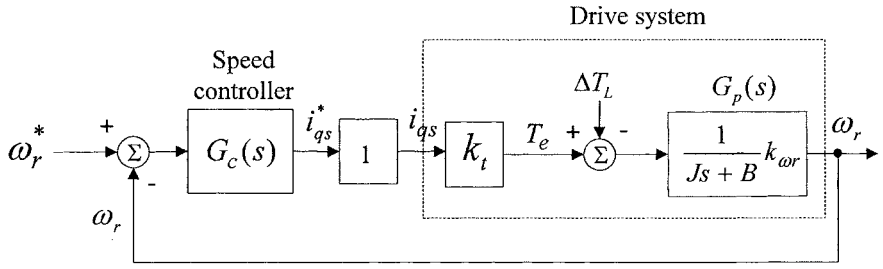

(b)

Fig. 1. An indirect-field-oriented induction motor drive. (a) System configuration. (b) Control system block diagram.

lowing controller is designed at the nominal case according to the estimated plant model and prescribed tracking and regulation speed responses. Then, an output feedback VSS controller is proposed and used to reduce the effects of system parameter changes on the desired speed responses. The proposed VSS controller is easy to implement, since only the plant output information is needed for the control. The inherent chattering problem during the steady-state period is eliminated through applying the boundary-layer method. The theoretical basis of the proposed VSS controller is derived in detail, and its effectiveness is demonstrated by some simulation and measured results.

II. IFO Induction Motor Drive

The block diagram of an IFO induction motor drive system is shown in Fig. 1(a). It consists of an outer speed controller loop, indirect-field-orientation mechanism, current-controlled pulsewidth-modulation (PWM) voltage-source inverter (VSI), and induction motor. In order to test the load regulation characteristics of the drive system, the induction motor is mechanically coupled to a dc generator with switched load resistances. The induction motor used here is 2 P, 5.4 A, 120 V, and 2000 r/min, having the following single-phase equivalent circuit parameters:

$$\begin{aligned} R_s &= 1.1\ \Omega \\ R_r &= 1.3\ \Omega \\ L_s &= 0.144\ \text{H} \\ L_r &= 0.144\ \text{H} \\ L_m &= 0.136\ \text{H}. \end{aligned} \tag{1}$$

The meanings of the above parameters are clear from [1].

For an ideally decoupled induction motor, its rotor flux linkage is forced to be aligned with the d axis of sthe ynchronously rotating frame, i.e.,

$$\lambda_{qr} = 0 \quad \text{and} \quad \frac{d\lambda_{qr}}{dt} = 0 \tag{2}$$

λ_{qr} being the q-axis rotor flux linkage. Basically, the field-orientation control is a kind of predictive control. It can be derived that the d-axis rotor flux linkage λ_{dr} and the estimate of slip angular speed $\hat{\omega}_{sl}$ required to achieve the ideal decoupling are as follows:

$$\lambda_{dr} = \frac{L_m R_r/L_r}{p + R_r/L_r}\, i_{ds}^* \quad \hat{\omega}_{sl} = \frac{L_m R_r}{\lambda_{dr} L_r}\, i_{qs}^* \tag{3}$$

where $i_{ds}^*(i_{qs}^*)$ is the $d(q)$-axis stator current command and $p = d/dt$. Generally, the electrical time constant L_r/R_r in (3) is much smaller than the mechanical time. If neglected, we could further get

$$\lambda_{dr} = L_m i_{ds}^* \quad \hat{\omega}_{sl} = \frac{R_r i_{qs}^*}{L_r i_{ds}}. \tag{4}$$

For an ideal field-oriented induction motor drive, the torque equation becomes

$$T_e = \left(\frac{3}{4} P \frac{L_m^2}{L_r}\, i_{ds}^*\right) i_{qs}^* \triangleq k_t i_{qs}^* = T_L + B\omega_r + J\frac{d}{dt}\,\omega_r \tag{5}$$

where P is the number of poles, $B \triangleq B_{\text{motor}} + B_{\text{load}}$ is the total damping factor, and $J \triangleq J_{\text{motor}} + J_{\text{load}}$ is the total mechanical inertia constant. Thus, the dynamic behavior of an ideal IFO induction motor drive shown in Fig. 1(a) can be reasonably represented by the control system block diagram drawn in Fig. 1(b), in which, k_t is the torque constant defined in (5), $k_{\omega r}$(=0.009 55 here) denotes the conversion ratio from the measured speed to the sensed signal, and the parameters of the plant $G_P(s)$ are defined as

$$a \triangleq \frac{B}{J} \quad b \triangleq \frac{1}{J}\, k_{\omega r}. \tag{6}$$

Although the parameters of the dynamic model blocks shown in Fig. 1(b) can be determined by the physical derivation introduced above, their accurate values are rather difficult to obtain. It follows that the estimation method [18] is employed as an alternative, and the following estimated results:

$$\begin{aligned} k_t &= 0.759 \\ a &= 0.567, \\ b &= 70.68 \times 0.009\,55 = 0.675 \end{aligned} \tag{7}$$

will be used for making the controller design.

III. Configuration and Problem Statement of the Proposed VSS Speed Controller

The system configuration of the proposed VSS speed controller for an IFO induction motor drive is shown in Fig. 2(a). It basically consists of the induction motor drive, a 2DOF controller, a linear model-following controller, and a VSS controller. First, at the nominal operating condition, a 2DOF controller is designed based on the known plant model to let the motor drive possess the desired tracking and regulation speed control performance. Then, a reference model, which is equal to the closed-loop transfer function of the motor drive using the designed 2DOF controller, is defined, and the linear model-following control gains are found.

As the parameter changes of motor and mechanical load occur, the speed responses of the detuned induction motor drive will deviate from the prescribed ones. A control force $u_v = G_{\text{vss}}(e_o, t)e_o$ is generated by the proposed VSS controller to automatically compensate this performance degradation. In the proposed VSS controller, the boundary-layer method is used for eliminating the chattering when entering the static period.

IV. 2DOFLMFC

A. Quantitative Design of the 2DOF Speed Controller

For directly incorporating the tracking and regulation speed control specifications of the motor drive into the controller design stage, the 2DOF controller shown in Fig. 2(b) is employed. It consists of a feedback controller $G_c(s)$ and a command feedforward controller $G_f(s)$

$$G_c(s) = k_p + \frac{k_i}{s} \quad G_f(s) = \frac{c_1 s + c_0}{d_1 s + d_0}. \tag{8}$$

For the ease of deviation, let

$$G_c'(s) = k_t G_c(s) = k_p' + \frac{k_i'}{s} \tag{9}$$

where

$$k_p' = k_t k_p \quad k_i' = k_t k_i. \tag{10}$$

While $G_c(s)$ is emphasized in dealing with the load regulation control, $G_f(s)$ is arranged to modify the command, such that the desired tracking response is obtained. To achieve this goal, the denominator of $G_f(s)$ is chosen to cancel the numerator of $G_{dr}^*(s) \triangleq \Delta\omega_r(s)/\Delta\omega_d(s)|_{\Delta T_L=0}$, and the numerator of $G_f(s)$ is designed to meet the prescribed step command tracking response. Accordingly, the structure of $G_f(s)$ can be rewritten as

$$G_f(s) = \frac{c_1 s + c_0}{d_1 s + d_0} = \frac{c_1 s + c_0}{k_p' b s + k_i' s} \tag{11}$$

and the closed-loop tracking transfer function can be expressed as

$$\begin{aligned} G_{dr}(s) &\triangleq \left.\frac{\Delta\omega_r(s)}{\Delta\omega_d^*(s)}\right|_{\Delta T_L=0} \\ &= G_f(s) G_{dr}^*(s) \\ &= \frac{c_1 s + c_0}{(s+\mu_1)(s+\mu_2)} \\ &= \frac{h_1}{(s+\mu_1)} + \frac{h_2}{(s+\mu_2)} \end{aligned} \tag{12}$$

where

$$\mu_1 + \mu_2 = a + k_p' b \quad \mu_1 \mu_2 = k_i' b. \tag{13}$$

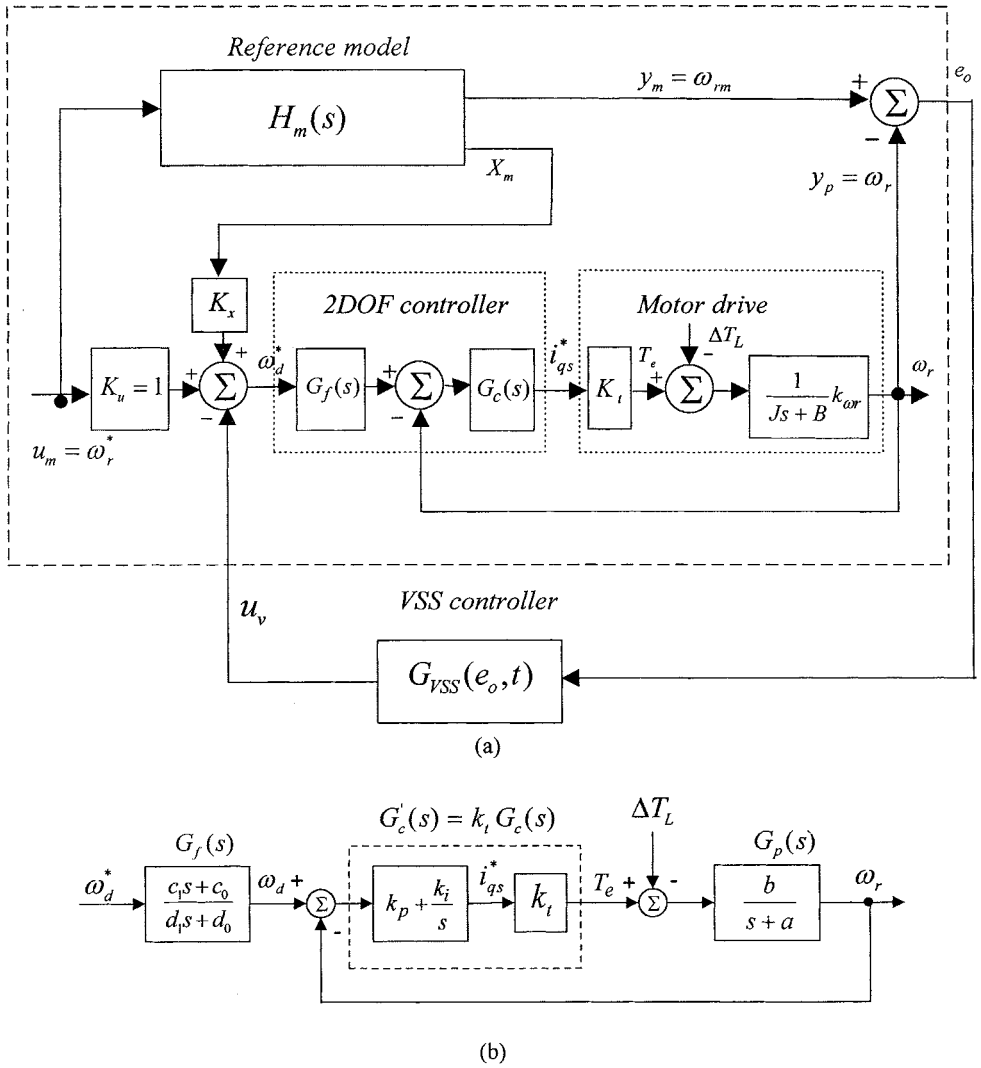

Fig. 2. (a) System configuration of the proposed VSS speed controller for the IFO induction motor drive. (b) Detailed configuration of the 2DOF controller.

Generally speaking, the performance requirements of a motor drive can be listed as follows.

1) The step tracking and regulation speed responses should contain no steady-state error.
2) The step tracking speed response should contain no overshoot.
3) The response time $= t_{\rm re}$, which is designed as the time that the unit-step tracking speed response rises from 0% to 90% of its steady-state value.
4) The maximum speed dip due to unit-step load change ($\Delta T_L = 1N - m$) is

$$\Delta\omega_{d\max}. \tag{14}$$

The formulations associated with the control requirements listed above can be derived to be [4]

$$f_1(\mu_1, \mu_2, h_1, h_2) = \frac{h_1}{\mu_1} + \frac{h_2}{\mu_2} - 1 = 0 \tag{15}$$

$$f_2(\mu_1, \mu_2, h_1, h_2) = h_1 - \left(\frac{\mu_1}{\mu_2}\right)^{1/2}, \qquad h_2 = 0 \tag{16}$$

$$f_3(\mu_1, \mu_2, h_1, h_2) = 0.9 - \left[\frac{h_1}{\mu_1}(1 - e^{-\mu_1 t_{\rm re}}) + \frac{h_2}{\mu_2}(1 - e^{-\mu_2 t_{\rm re}})\right] = 0 \tag{17}$$

$$f_4(\mu_1, \mu_2, h_1, h_2) = \Delta\omega_{d\max} - \frac{b}{\mu_1 - \mu_2} \cdot \left(e^{-(\mu_1/\mu_1 - \mu_2)\ \ln(\mu_1/\mu_2)} - e^{-(\mu_2/\mu_1 - \mu_2)\ \ln(\mu_1/\mu_2)}\right) = 0. \tag{18}$$

Having solved the variables μ_1, μ_2, h_1, and h_2 in (15)–(18), the parameters of $G_c(s)$ and $G_f(s)$ can be derived from (11)–(13)

$$\begin{aligned} c_0 &= h_1\mu_2 + h_2\mu_1 \\ c_1 &= h_1 + h_2 \\ d_0 &= \mu_1\mu_2 \\ d_1 &= \mu_1 + \mu_2 - a \end{aligned} \tag{19}$$

$$k_p' = \frac{\mu_1 + \mu_2 - a}{b} \quad k_i' = \frac{\mu_1\mu_2}{b}. \tag{20}$$

Design Example: The control specifications of this IFO induction motor drive are prescribed to be those listed in (14) with $t_{\rm re} = 0.3$ s and $\Delta\omega_{d\max} = 30$ r/min. Using the estimated plant dynamic model parameters listed in (7) and the given specifications, the parameters of $G_c(s)$ and $G_f(s)$ are found following the proposed design procedure to be

$$\begin{aligned} c_0 &= 66.2451 \\ c_1 &= 8.1391 \\ d_0 &= 66.2451 \\ d_1 &= 16.1254 \\ k_p &= 31.4750 \\ k_i &= 129.3029. \end{aligned} \tag{21}$$

The simulation results (not shown here) show that the given specifications are completely satisfied.

B. LMFC

The design of an output feedback LMFC has been introduced in detail in [5], and only a brief description is given here. Suppose that the plant to be controlled and the selected reference model can be expressed as

$$\dot{x}_p = A_p x_p + B_p u_p \quad y_p = C_p x_p \tag{22}$$

$$\dot{x}_m = A_m x_m + B_m u_m \quad y_m = C_m x_m = C_p x_m \tag{23}$$

where $x_p \in R^n$, $x_m \in R^n$, $u_p \in R^p$, $u_m \in R^p$, $y_p \in R^q$, $y_m \in R^q$. For the following control law:

$$u_p = K_x x_m + K_u u_m + K_e e_o \tag{24}$$

$$e_o \triangleq y_m - y_p = C_p(x_m - x_p) \triangleq C_p e \tag{25}$$

it is found that if A_m, B_m, K_x, K_u, and K_e are chosen to let $(A_p - B_p K_e C_p)$ be a Hurwitz matrix and $K_x = B_p^+(A_m - A_p)$, $K_u = B_p^+ B_m$, and $B_p^+ = (B_p^T B_p)^{-1} B_p^T$, then the output of the controlled plant will follow the output of reference model asymptotically.

In real operation, the actual plant parameters may deviate significantly from the nominal ones used in the controller design. The LMFC with fixed gains fails to yield control performance with parameter-insensitive characteristics. To solve this problem, a VSS controller is employed to generate an adaptation signal u_{pa} to compensate the performance deviation.

Reference Model Selection: From the designed results presented in Section IV-A, one can find the tracking transfer function of the motor drive controlled by the 2DOF controller (2DOFC):

$$\begin{aligned} H_m(s) = G_{dr}(s) &\triangleq \left.\frac{\Delta\omega_r(s)}{\Delta\omega_d^*(s)}\right|_{\Delta T_L = 0} \\ &= \frac{8.1391s + 66.2451}{s^2 + 16.6924s + 66.2451}. \end{aligned} \tag{26}$$

The state-space expression of (26) can be found to be

$$\begin{aligned} A_m &= \begin{bmatrix} 0 & 1 \\ -66.2451 & -16.6924 \end{bmatrix} \\ B_m &= \begin{bmatrix} 0 \\ 1 \end{bmatrix} \\ C_m &= [66.2451 \;\; 8.1391]. \end{aligned} \tag{27}$$

$H_m(s)$ is chosen as a reference model since it represents the desired tracking response at the nominal case. Since the transfer functions of the controlled motor drive by the 2DOF controller at the nominal case and the reference model are identical, it follows from (25) that $K_x = 0$ and $K_u = 1$.

V. Proposed VSS Speed Controller

For the control system shown in Fig. 1, the dynamic behavior of the model-following tracking error e_o due to the system uncertainty and the control yielded by the VSS controller can be implicitly modeled in Fig. 3 and expressed by

$$\begin{aligned} \ddot{e}_o(\dot{e}_o, e_o, t) &= \overline{f}(\dot{e}_o, e_o, t) + \Delta f(\dot{e}_o, e_o, t) - u_v(t) \\ &= \Delta f(\dot{e}_o, e_o, t) - u_v(t) \end{aligned} \tag{28}$$

where the nominal dynamic $\overline{f}$ is zero since the 2DOFLMFC has been properly designed at the nominal case to let the tracking error always be zero. The uncertain dynamic function Δf denotes the error dynamic caused by system parameter variations, and $u_v(t)$ denotes the control effect yielded by the proposed VSS controller to eliminate the model-following tracking error as the operating conditions and system parameters are deviated from those at the nominal case. In the design of the proposed VSS controller, the desired error vector is set as $[\dot{e}_{od}, e_{od}]^T = [0, 0]$. In addition, it also lets $\ddot{e}_{od} = 0$.

A. Sliding-Mode Control Without Chattering Suppression

For achieving sliding-mode control, a switching line and a sliding-mode control law are chosen as

$$\sigma = \dot{e}_o + \lambda e_o \tag{29}$$

$$\begin{aligned} u_v &= -\lambda\dot{e}_o - D\left(|\Delta f| + \eta\right)\mathrm{sgn}(\sigma) \\ &\triangleq u_v^c + u_{v1}^d, \qquad D \geq 0; \quad \eta \geq 0. \end{aligned} \tag{30}$$

The continuous control u_v^c is a compensation signal, which helps to reduce the model-following error during the initial transient period and, thus, bring the phase portrait of the error dynamic system toward the switching line, and the discontinuous control u_{v1}^d is actuated to achieve the sliding-mode control. The detailed configuration of the proposed VSS controller is shown in Fig. 3.

In realizing the control law listed in (30), the estimate of Δf is found from (28)

$$\Delta\hat{f} = -u_v + \ddot{e}_o \tag{31}$$

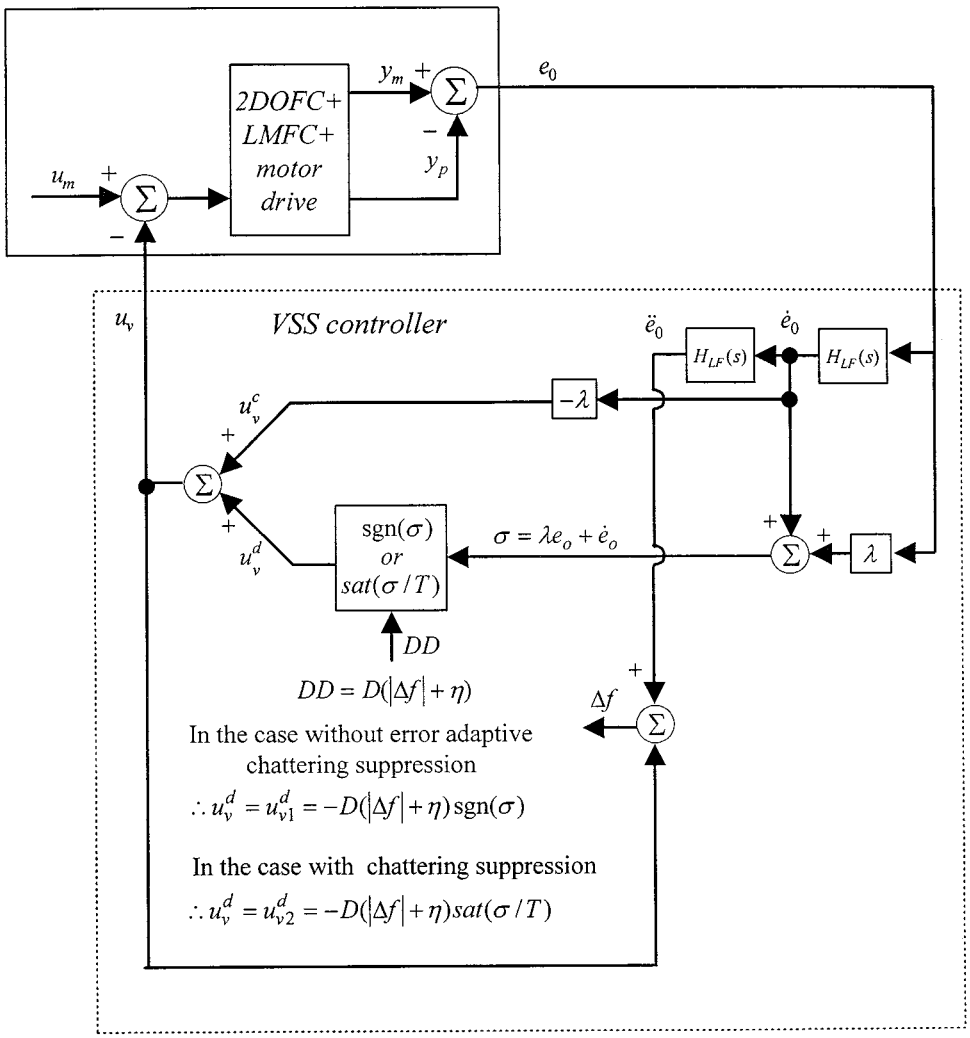

Fig. 3. Detailed configuration of the proposed VSS controller.

and $\dot{e}_o$ and $\ddot{e}_o$ are obtained from e_o through a practical differentiator, which is implemented using a low-pass filter

$$H_{\mathrm{LF}}(s) = \frac{s}{(1+\mu_1 s)(1+\mu_2 s)}. \tag{32}$$

Although $H_{\mathrm{LF}}(s)$ serves as a differentiator within the main dynamic frequency range, it will become a low pass filter for the high-frequency noises. The magnitude of the chosen discontinuous control u_{v1}^d will gradually decrease accompanying with the convergence of tracking error. It follows that the switching of control action is greatly reduced, and moreover, the steady-state error of e_o is not existed.

As the operating condition and/or the system parameters deviate from those of nominal case, to let the model following error be quickly decayed to zero along the chosen sliding line, it is required that the following sufficient sliding condition is satisfied:

$$\frac{1}{2}\frac{d}{dt}\sigma^2(\dot{e}_o, e_o, t) = \sigma\dot{\sigma} = \dot{\sigma}|\sigma|\mathrm{sgn}(\sigma) \le -\eta|\sigma|, \quad \eta \ge 0. \tag{33}$$

By substituting (28)–(30) into (33), one can derive:

$$\begin{aligned}\frac{1}{2}\frac{d}{dt}\sigma^2(\dot{e}_o, e_o, t) &= \sigma\dot{\sigma} = (\ddot{e}_o + \lambda\dot{e}_o)\sigma = (\Delta f + u_v + \lambda\dot{e}_o)\sigma \\ &= (\Delta f - \lambda\dot{e}_o + \lambda\dot{e}_o - D(|\Delta f| + \eta)\,\mathrm{sgn}(\sigma))\,\sigma \\ &= (\Delta f - D(|\Delta f| + \eta)\,\mathrm{sgn}(\sigma))\,\sigma \\ &= (\Delta f\sigma - |\Delta f||\sigma|) + |\Delta f||\sigma| - D|\Delta f||\sigma| - \eta D|\sigma| \\ &\le (-D|\Delta f| - \eta D + |\Delta f|)\,|\sigma|. \end{aligned} \tag{34}$$

It is obvious from (34) that the sufficient condition to make inequality of (33) be satisfied is:

$$D(|\Delta f| + \eta) \ge |\Delta f|. \tag{35}$$

Comments: Some properties of the proposed VSS controller corresponding to (28)–(35) can be predicted:

i) As the disturbance is suddenly occurred, the compensation term u_v^c in (30) will be dominant during the initial transient period. But when the phase portrait $(e_o, \dot{e}_o)$ is forced to approach the neighborhood of switching line,

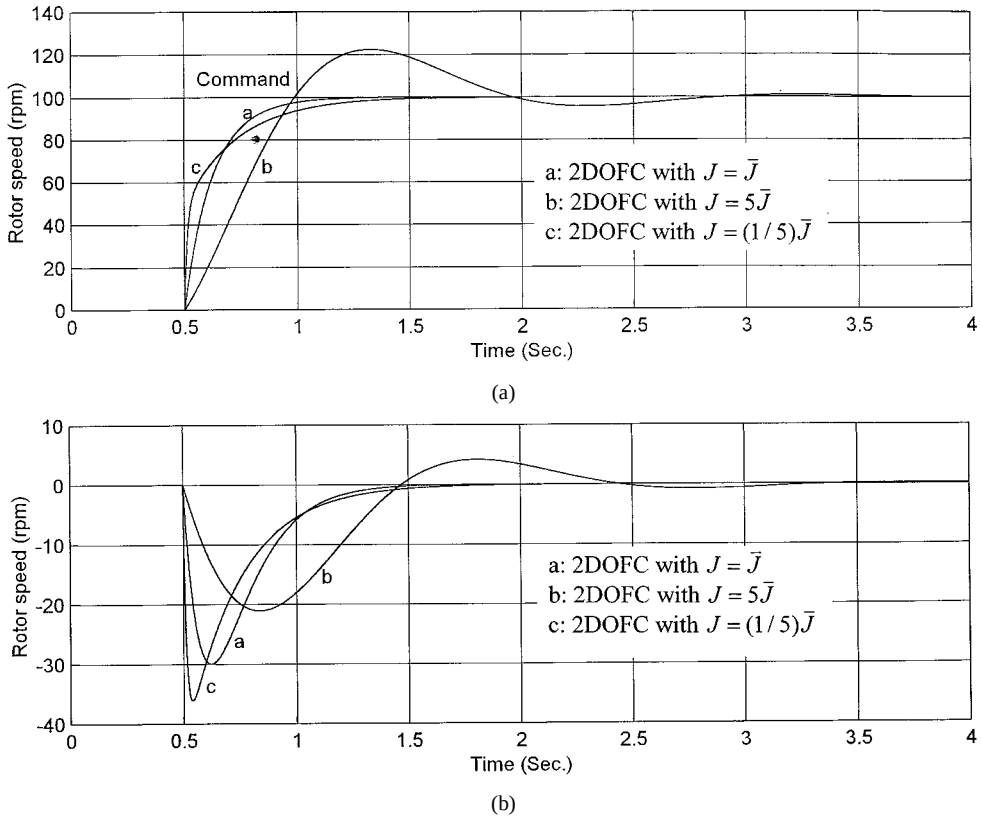

Fig. 4. (a) Simulated rotor speeds of the 2DOF controller due to the step speed command $\Delta\omega_d^*$ (100 r/min) change at $\omega_{r0} = 1000$ r/min, $R_{L0} = 77.6\ \Omega$ with $J = \overline{J}$, $J = 5\overline{J}$, and $J = 1/5\overline{J}$. (b) Simulated rotor speed responses due to the step load torque $\Delta T_L = 1$ N·m at the same conditions as (a).

the condition of (35) will be satisfied automatically and then the error dynamic system enters the sliding control mode by the control u_{v1}^d with invariance property of VSS. The parameter D is used to adjust the sensitivity of switching behavior.

ii) Since no soft switching control strategies are employed for the discontinuous control u_{v1}^d in (30), the chattering is always existed during the static period. The extent of chattering is dependent on the chosen parameters D and η.

B. Sliding Mode Control With Chattering Suppression

For eliminating the chattering phenomena existed in the VSS controller introduced above, the control law in (30) is modified using the simple boundary-layer method as follows:

$$u_v = -\lambda\dot{e}_o - D\left(|\Delta f| + \eta\right) sat\left(\frac{\sigma}{T}\right) \triangleq u_v^c + u_{v2}^d, \qquad D \geq 0; \quad \eta \geq 0; \quad \sigma = \dot{e}_o + \lambda e_o \tag{36}$$

where the saturation function is defined as:

$$sat\left(\frac{\sigma}{T}\right) = \begin{cases} \operatorname{sgn}\left(\frac{\sigma}{T}\right), & \text{if } \left|\frac{\sigma}{T}\right| \geq 1, \\ \frac{\sigma}{T}, & \text{if } \left|\frac{\sigma}{T}\right| < 1, \end{cases} \qquad T > 0 \tag{37}$$

with T being half of the width of the boundary layer.

Comments:

i) The phase portrait dynamic behavior governed by the two control parts u_v^c and u_{v2}^d is similar to those described in Section V-A .

ii) Due to the incorporation of the boundary layer, the chattering is eliminated in steady-state. The small stead-state error caused by boundary layer will be eliminated by the integration action existed in the feedback controller of the 2DOFC.

C. Simulation Results

1) 2DOF Controller: The simulated rotor speeds of the 2DOF controller due to a step speed command change of $\Delta\omega_d^* = 0.1$ V (100 rpm) at ($\omega_{r0} = 1000$ rpm, $R_{L0} = 77.6\ \Omega$) with inertia constants $J = \overline{J}$, $J = 5\overline{J}$ and $J = 1/5\overline{J}$ are shown in Fig. 4(a). At the same conditions, the simulated rotor speed responses due to a step load torque change of $\Delta T_L = 1N - m$ are shown in Fig. 4(b). The results shown in Fig. 4(a) and (b) clearly indicate that as the variations of system parameters occurred, the responses deviate significantly from those of nominal case.

2) Sliding Mode Controller Without Chattering Suppression: The sliding line and the control law of the proposed controller listed in (29) and (30) are chosen as:

$$\sigma = \dot{e}_o + \lambda e_o = \dot{e}_o + e_o \tag{38}$$

$$u_v = -\lambda\dot{e}_o - D\left(|\Delta f| + \eta\right)\operatorname{sgn}(\sigma) = -\dot{e}_o - \left(|\Delta f| + 0.1\right)\operatorname{sgn}(\sigma) \tag{39}$$

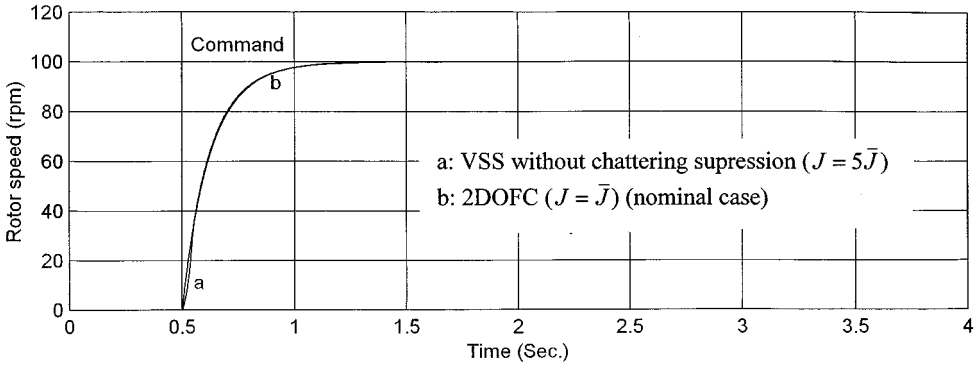

(a)

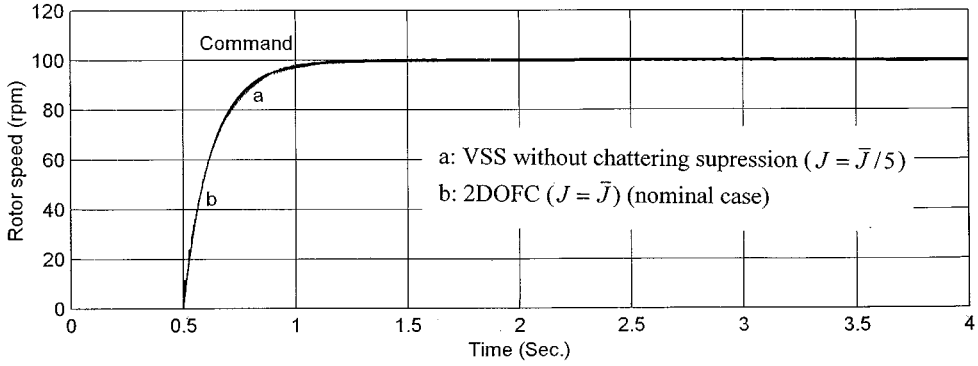

(b)

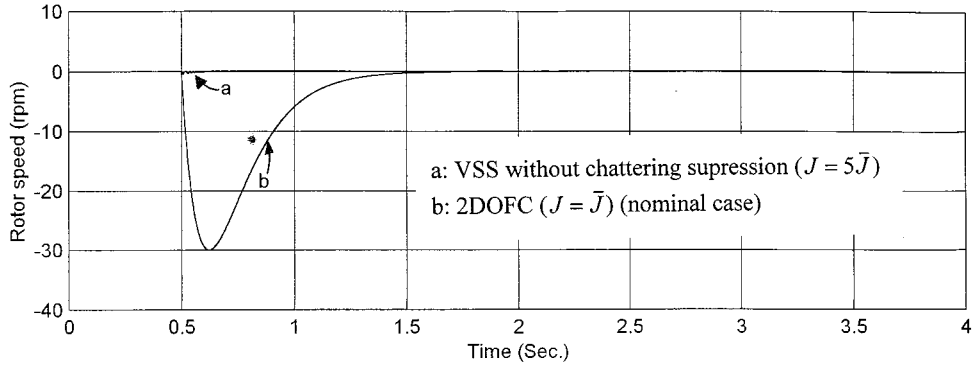

(c)

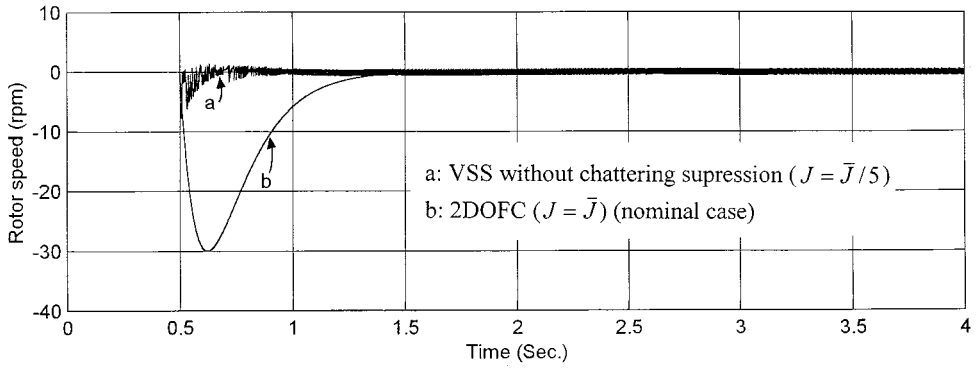

(d)

Fig. 5. Simulated results of the proposed VSS controller without chattering suppression at the same conditions as Fig. 4. (a) Step tracking responses with $J = 5\overline{J}$. (b) Step tracking responses with $J = 1/5\overline{J}$. (c) Step regulation response with $J = 5\overline{J}$. (d) Step regulation response with $J = 1/5\overline{J}$.

where $\lambda = 1$, $D = 1$ and $\eta = 0.1$ are chosen. The low pass filter in (32) to get the derivative of error vector is set as:

$$H_{\mathrm{LF}}(s) = \frac{s}{0.225s^2 + 0.3s + 1}. \tag{40}$$

For the same conditions as those in Fig. 4, the simulated step speed tracking responses with $J = 1/5\overline{J}$ and $J = 5\overline{J}$ of the proposed VSS controller without chattering suppression are shown in Fig. 5(a) and (b), respectively. As to the step regulation

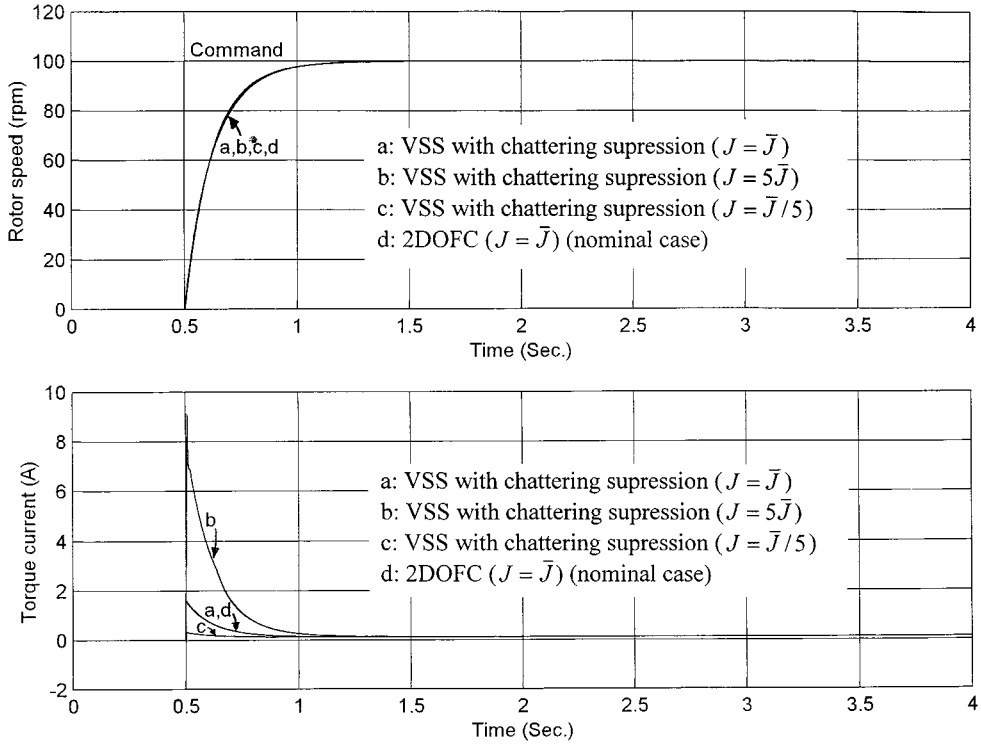

(a)

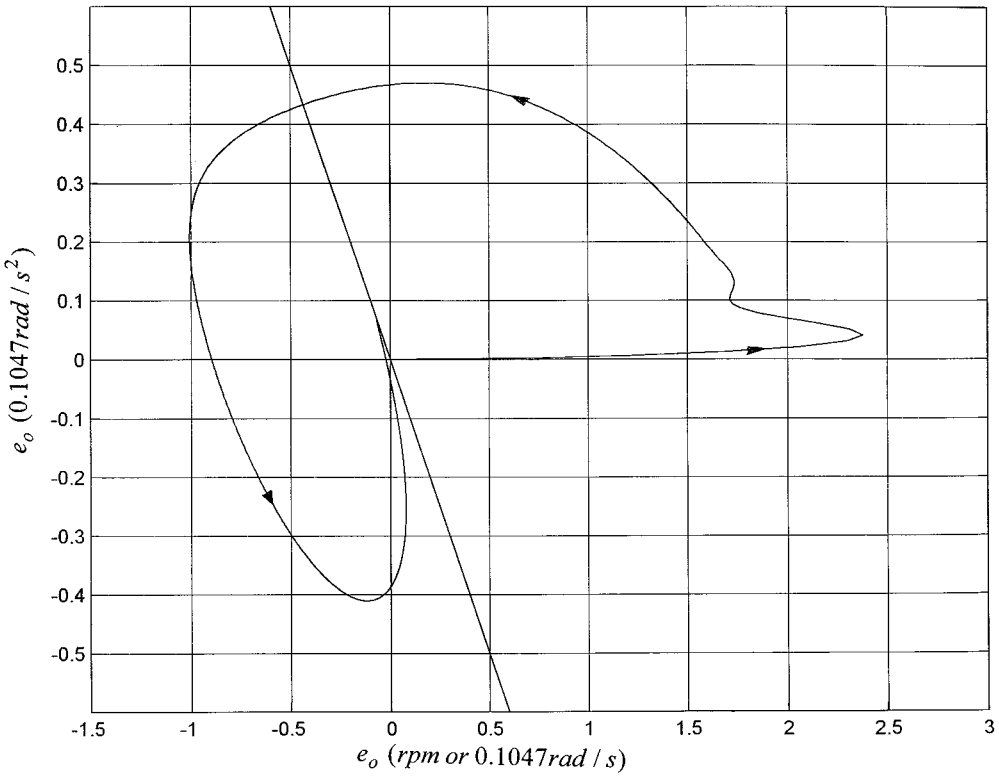

(b)

Fig. 6. Simulated rotor speeds and torque currents i_{qs}^* of the proposed VSS controller with chattering suppression at the same conditions as Fig. 4. (a) Step tracking responses with $J = 1/5\overline{J}$, $J = \overline{J}$, and $J = 5\overline{J}$. (b) Phase portrait $(e_o, \dot{e}_o)$ with $J = 5\overline{J}$.

response, Fig. 5(c) and (d) shows the speed responses with $J = 1/5\overline{J}$ and $J = 5\overline{J}$. The results shown in Fig. 5(a)–(d) confirm the correct operation of the designed VSS controller. However, unfortunately, the chattering phenomena are observed from the results.

3) Sliding-Mode Controller With Chattering Suppression: The parameters of the proposed VSS control law in (36) are chosen to be

$$D = 1 \quad \eta = 0.1 \quad \lambda = 1 \quad T = 0.003. \tag{41}$$

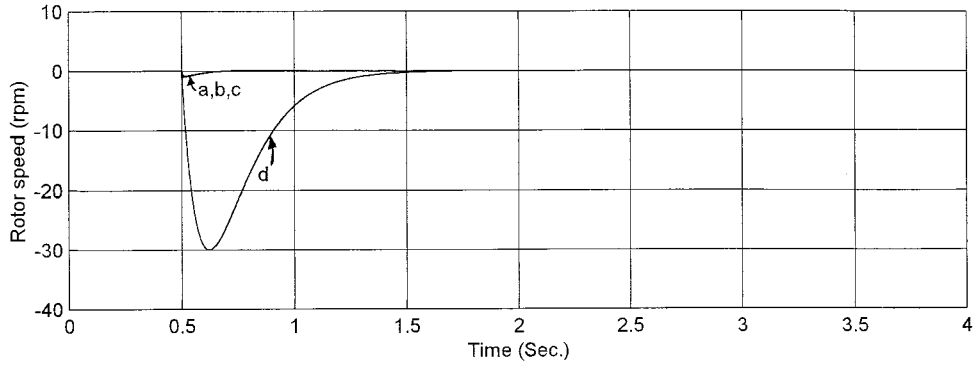

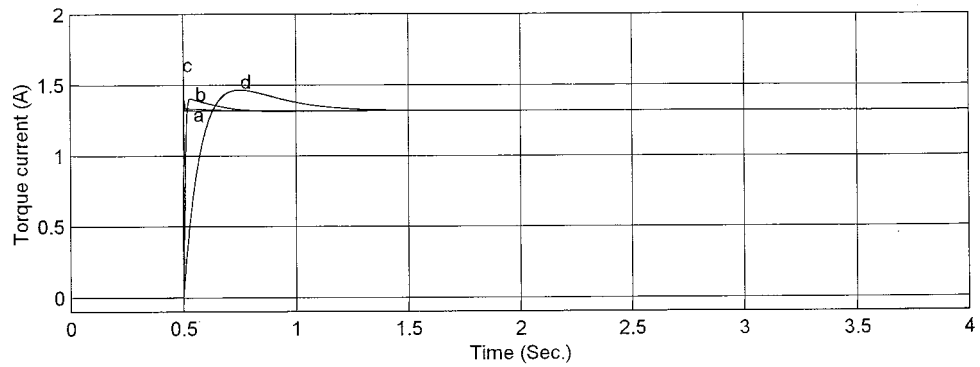

(a)

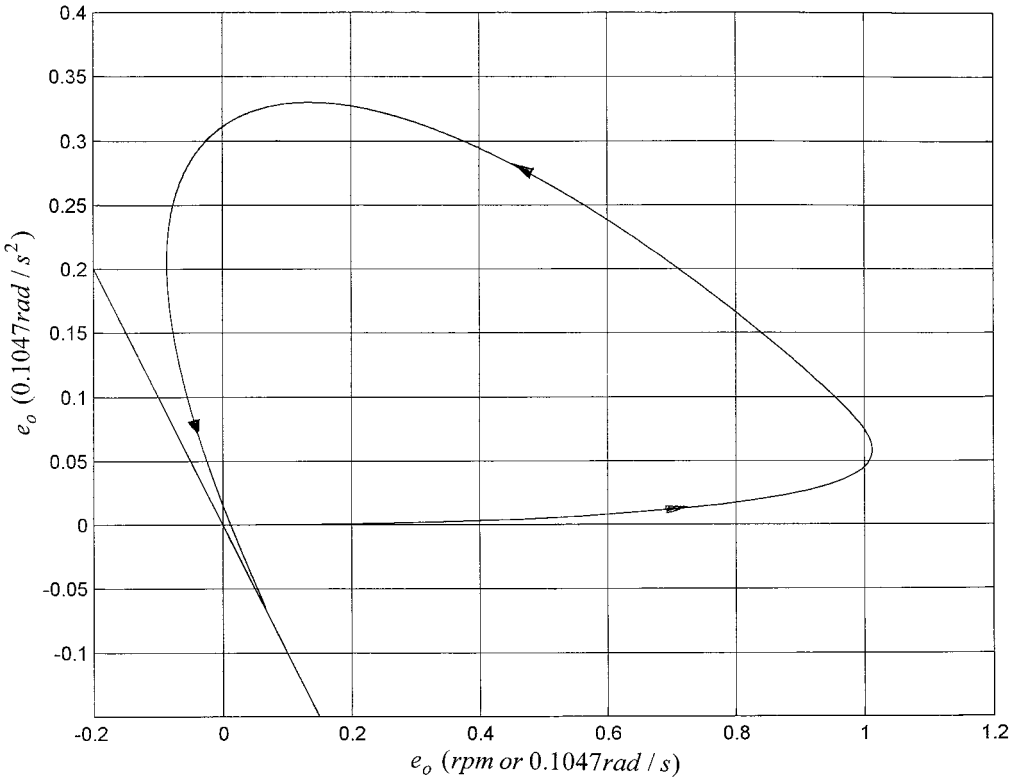

(b)

Fig. 7. Simulated rotor speeds and torque currents i_{qs}^* of the proposed VSS controller with chattering suppression at the same conditions as Fig. 4. (a) Step regulation responses with $J = 1/5\overline{J}$, $J = \overline{J}$, and $J = 5\overline{J}$. (b) Phase portrait $(e_o, \dot{e}_o)$ with $J = 5\overline{J}$.

For the same conditions as those in Fig. 4(a) and (b), the simulated tracking step speed responses and the resulting torque currents with $J = 1/5\overline{J}$, $J = \overline{J}$, and $J = 5\overline{J}$ of the proposed VSS controller are shown in Fig. 6(a). The corresponding phase portrait $(e_o, \dot{e}_o)$ with $J = 5\overline{J}$ is shown in Fig. 6(b). As to the regulation responses, Fig. 7(a) shows the speed and torque current responses at the cases of $J = 1/5\overline{J}$, $J = \overline{J}$, and $J = 5\overline{J}$. The phase portrait $(e_o, \dot{e}_o)$ with $J = 5\overline{J}$ is shown in Fig. 7(b). From

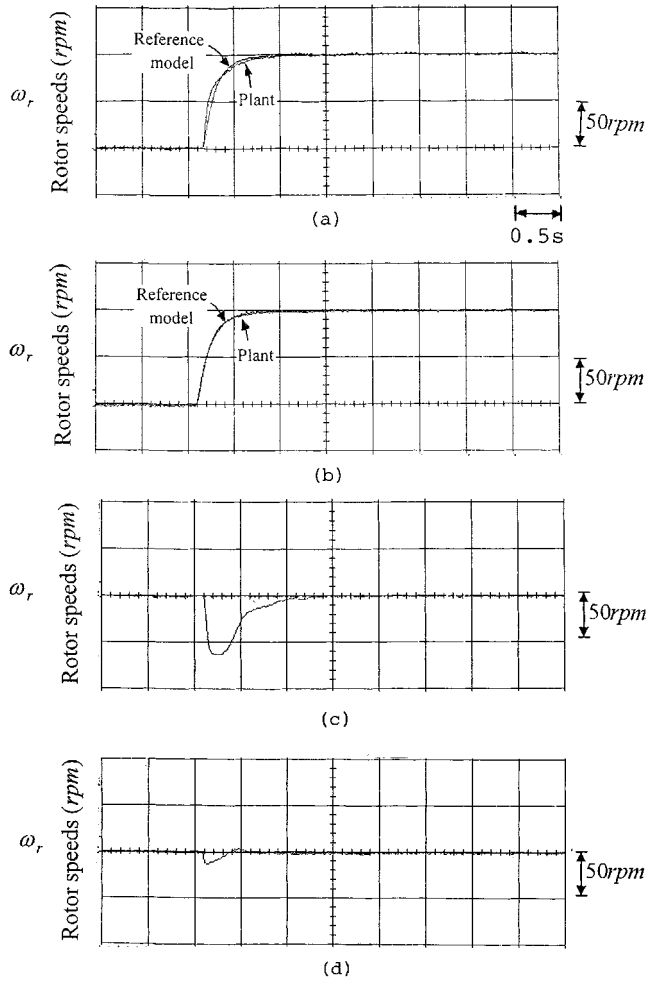

Fig. 8. (a) Measured rotor speeds due to step command change (1000 → 1100 r/min at nominal case ($\omega_{r0} = 1000$ r/min, $R_{L0} = 77.6\ \Omega$, 2.7 A) by only the 2DOFC. (b) Proposed VSS controller with chattering suppression at the same conditions as (a). (c) Measured rotor speeds due to step load resistance change ($77.6 \rightarrow 27.4\ \Omega$) at nominal case by only the 2DOFC. (d) Proposed VSS controller with chattering suppression at the same conditions as (c).

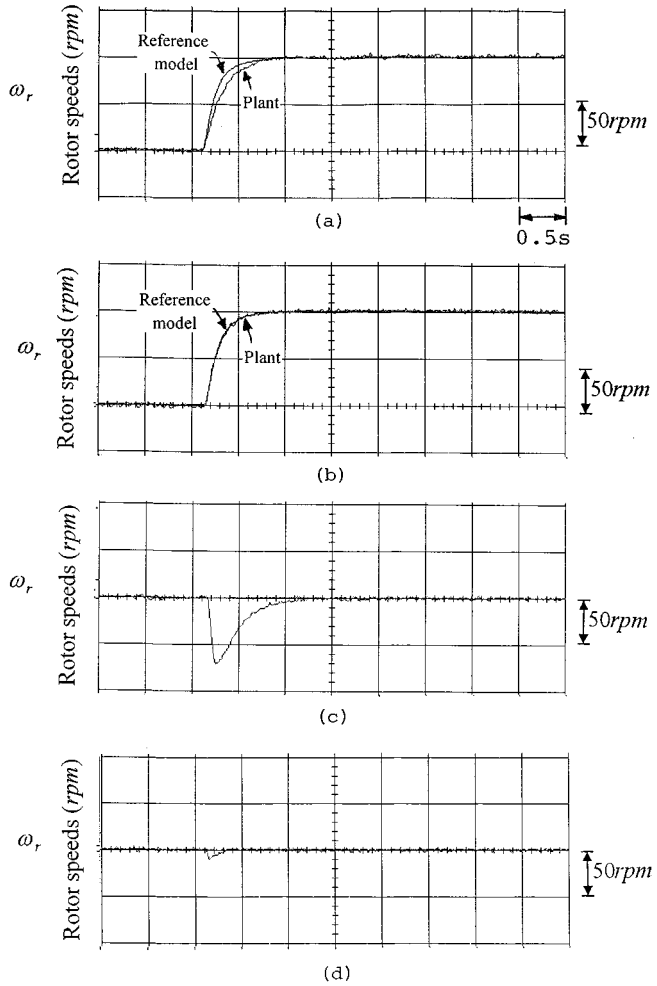

Fig. 9. (a) Measured rotor speeds due to step command change (2000 → 2100 r/min) at $\omega_r = 2000$ r/min, $R_L = 52.3\ \Omega$ by only the 2DOFC. (b) Proposed VSS controller with chattering suppression at the same conditions as (a). (c) Measured rotor speeds due to step load resistance change (77.6 → 52.3 Ω) at $\omega_r = 2000$ r/min, $R_L = 77.6\ \Omega$ by only the 2DOFC. (d) Proposed VSS controller with chattering suppression at the same conditions as (c).

Figs. 6 and 7, one can observe that the large initial transient model-following error is quickly reduced by the continuous control effort, as the value of $s\dot{s}$ becomes negative, the reaching condition is satisfied and, thus, the corresponding phase portrait approaches the sliding line and within the boundary layer. Then, the error converges to zero asymptotically without chattering, owing to the boundary layer and the integration action in the 2DOFC. Good model-following tracking responses at all cases are observed from these results, and the resulting regulation responses are also much better (in both speed dip and restore time) than those obtained by the 2DOFC only.

D. Experimental Results

The proposed control system shown in Figs. 2 and 3 is digitally implemented in a personal computer using C language. All the blocks, including the 2DOFC, LMFC, and VSS controller are transformed into digital control algorithms by bilinear transform method.

The IFO induction motor drive with the designed 2DOFC is normally operated at the chosen nominal case ($\omega_{r0} = 1000$ r/min, $R_{L0} = 77.6\ \Omega$, 2.7 A). The measured rotor speed responses due to the step command change (1000 → 1100 r/min) without and with the proposed VSS controller with chattering suppression are shown in Fig. 8(a) and (b). The measured rotor speed responses due to the step load resistance change (77.6 → 27.4 Ω) at the nominal case without and with the proposed VSS controller with chattering suppression are shown in Fig. 8(c) and (d). From the results in Fig. 8(c) and the torque constant listed in (7), one can find that the maximum speed dip of 62 r/min corresponds to the step load torque $2.55 \times 0.759 = 1.935$ N·m ($\Delta i_{qs}^* \approx 2.55$ A), i.e., a 1-N·m load torque change causes a maximum speed dip of 32 r/min; this is rather close to those prescribed in Section IV-A. After employing the proposed VSS control, a much smaller speed dip with zero steady-state error for the same case is observed from the results shown in Fig. 8(d).

Because suitable equipment for changing the load inertia constant and damping ratio is not available, for the convenience of making a further test of the effectiveness of the proposed VSS controller under large plant parameter variations, the changes of flux current command i_{ds}^* from 3.3 A (the rated value) to 1.65

A and the rotor resistance R_r set in the field-orientation mechanism from 1.3 Ω (the nominal value) to 1.5 Ω are made as an alternative. In this detuned IFO induction motor drive, the measured rotor speed responses due to the step command change (2000 $\rightarrow$ 2100 r/min) at $\omega_r = 2000$ r/min and $R_L = 52.3\ \Omega$ without and with the proposed VSS controller are shown in Fig. 9(a) and (b). The measured rotor speed responses due to the step load resistance change (77.6 $\rightarrow$ 52.3 Ω) at $\omega_r = 2000$ r/min and $R_L = 77.6\ \Omega$ without and with the proposed VSS controller are shown in Fig. 9(c) and (d). The correctness and the performance improvements both in tracking and regulation responses of the proposed VSS controller can be clearly seen from the results given in Fig. 9(a)–(d).

VI. Conclusions

The development of a VSS controller for the speed control of an IFO induction motor drive has been presented. First, the motor drive is set up and its dynamic model is estimated from measurements. According to the estimated drive model at the nominal case, a 2DOFLMFC is quantitatively designed to match the prescribed control specifications. Then, an output feedback VSS controller is proposed to preserve the desired tracking and regulation control performance as the operating condition and parameter variations occur. In the proposed VSS controller, the boundary-layer method is employed to eliminate the steady-state chattering, which exists inherently in the traditional VSS controllers. The proposed VSS controller is easy to implement, since only the plant output is sensed. The simulation and measured results have confirmed that good and robust model-following tracking and load regulation speed responses are obtained by the designed VSS controller.

References

[1] B. K. Bose, *Power Electronics and AC Drives*. Englewood Cliffs, NJ: Prentice-Hall, 1986.

[2] R. Krishanan and A. S. Bharadwaj, "A review of parameter sensitivity and adaptation in indirect vector controlled induction motor drive system," in *Proc. IEEE PESC'90*, 1990, pp. 560–566.

[3] R. Krishnan and F. C. Doran, "Study of parameter sensitivity in high-performance inverter-fed induction motor drive systems," *IEEE Trans. Ind. Applicat.*, vol. 23, pp. 623–635, July/Aug. 1992.

[4] C. M. Liaw, "Design of a two-degree-of-freedom controller for motor drives," *IEEE Trans. Automat. Contr.*, vol. 37, pp. 1215–1220, Aug. 1992.

[5] Y. S. Kung and C. M. Liaw, "A fuzzy controller improving a linear model following controller for motor drives," *IEEE Trans. Fuzzy Syst.*, vol. 2, pp. 194–202, Aug. 1994.

[6] Y. S. Kung, M. Ouyang, and C. M. Liaw, "Adaptive speed control for induction motor drives using neural networks," *IEEE Trans. Ind. Electron.*, vol. 42, pp. 25–32, Feb. 1995.

[7] G. T. Kim, K. S. Kim, M. H. Park, C. T. Won, and D. S. Ahn, "Time optimal control for induction motor servo system," in *Proc. IEEE PESC'88*, 1988, pp. 1053–1062.

[8] F. J. Lin and C. M. Liaw, "Reference model selection and adaptive control for induction motor drives," *IEEE Trans. Automat. Contr.*, vol. 38, pp. 1594–1600, Oct. 1993.

[9] C. M. Liaw and F.J. Lin, "A robust speed controller for induction motor drives," *IEEE Trans. Ind. Electron.*, vol. 41, pp. 308–315, June 1994.

[10] U. Itkis, *Control Systems of Variable Structure*. New York: Wiley, 1976.

[11] J. Y. Hung, W. B. Gao, and J. C. Hung, "Variable structure control: A survey," *IEEE Trans. Ind. Electron.*, vol. 40, pp. 2–22, Feb. 1993.

[12] B. K. Bose, *Power Electronics and Variable Frequency Drives: Technology and Applications*. New York: IEEE Press, 1997.

[13] D. Driankov, H. Hellendoorn, and M. Reinfrank, *An Introduction to Fuzzy Control*. Berlin, Germany: Springer-Verlag, 1996.

[14] C. Y. Su and T. P. Leung, "A sliding mode controller with bound estimation for robot manipulators," *IEEE Trans. Robot. Automat.*, vol. 9, pp. 208–214, Feb. 1993.

[15] V. Parra-Vega, Y. H. Liu, and S. Arimoto, "Variable structure robot control undergoing chattering attenuation: Adaptive and nonadaptive cases," in *Proc. 1994 IEEE Conf. Robotics and Automation*, vol. 3, 1994, pp. 1824–1829.

[16] K. W. Lee, S. J. Lee, and K. K. Choi, "A model following variable structure controller," in *Proc. IEEE IECON'89*, 1989, pp. 330–334.

[17] A. S. Nouri, C. Mira, and P. Lopez, "Variable structure model reference adaptive control using only input and output measurement with two sliding surfaces," in *Proc. IEEE IECON'93*, 1993, pp. 2171–2177.

[18] C. M. Liaw, "System parameter estimation from sampled data," *Control Dyn. Syst.*, vol. 63, pp. 161–175, 1994.

Chang-Ming Liaw (S'88–M'89) was born in Taiwan, R.O.C., in 1951. He received the B.S. degree in electronic engineering from the Evening Department of the Tamkang College of Arts and Sciences, Taipei, Taiwan, R.O.C., and the M.S. and Ph.D. degrees in electrical engineering from National Tsing Hua University, Hsinchu, Taiwan, R.O.C., in 1979, 1981, and 1988, respectively.

In 1988, he joined the faculty of National Tsing Hua University as an Associate Professor of electrical engineering. Since 1993, he has been a Professor in the Department of Electrical Engineering. His research interests are power electronics and motor drives.

Yeong-May Lin was born in Maoli, Taiwan, R.O.C., in 1974. He received the B.S. and M.S. degrees from National Tsing Hwua University Hsinchu, Taiwan, R.O.C., in 1996 and 1998, respectively.

He is currently an Engineer with the R&D Department, AMBIT Microsystems Corporation, Hsinchu, Taiwan, R.O.C. His research interests include power electronics and motion control.

Kuei-Hsiang Chao was born in Tainan, Taiwan, R.O.C., in 1962. He received the B.S. degree from National Taiwan Institute of Technology, Taipei, Taiwan, R.O.C., and the M.S. and Ph.D. degrees from National Tsing Hua University, Hsinchu, Taiwan, in 1988, 1990, and 2000, respectively, all in electrical engineering.

He is currently an Associate Professor at National Chin Yi Institute of Technology, Taichung, Taiwan, R.O.C. His areas of research interest are motor drive control, computer-based control systems, and power electronics.